PERGAMON

International Journal of Heat and Mass Transfer 42 (1999) 2187–2198

International Journal of HEAT and MASS TRANSFER

Experimental analysis of unsteady heat and moisture transfer around a heated cylinder buried into a porous medium

R.E.S. Moya, A.T. Prata*, J.A.B. Cunha Neto

Department of Mechanical Engineering, Federal University of Santa Catarina, 88040-900 Florianópolis, SC, Brazil

Received 8 January 1997; in final form 15 September 1998

Abstract

An experimental analysis of heat and moisture transfer around a heated cylinder surrounded by an unsaturated soil is performed. The main motivation for the work is its application for high-voltage electrical power distribution in urban areas which, in general, makes use of underground cables. In the presence of electrical current, those cables generate heat that has to be dissipated through the surrounding soil in order to keep the cable temperature at safety levels; the cable operating temperature depends upon the soil ability to dissipate this heat. This is a complex phenomenon that involves several mechanisms of heat and moisture transfer. Experiments were performed for both constant and cyclic heating ranging from 8 to 80 W m^{-1}. Spatial as well as temporal temperature, heat flux and moisture content results are reported. Computations using a two-dimensional continuum model were also performed and a good agreement prevailed between numerical and experimental results. It was found that well-graded soils such as the one used in the present work have a great capacity for retaining moisture which is an important feature if high thermal conductivities around the heat source are desired.

Nomenclature

C soil thermal capacity
$D_{\theta w}$ isothermal water diffusivity
D_{Tw} thermal migration coefficient
$D_{\theta v}$ isothermal vapor diffusivity
F_o dimensionless time (Fourier number)
h_{lv} latent heat of vaporization
K_g hydraulic conductivity
k_{sat} saturation permeability
q' heat flux per unit cylinder length
r_c cylinder radius
S_r saturation degree at critical moisture content
T temperature
T^* dimensionless temperature
t time
T_i soil initial temperature.

Greek symbols

α_d soil thermal diffusivity
λ^* soil apparent thermal conductivity
θ volumetric moisture content
ρ_g density of the grain
ρ_l density of liquid water
ρ_s density of dry soil.

1. Introduction

An experimental program is conducted to investigate the transient response of a wet soil heated by a cylinder. The motivation for the work comes from its application to underground power cables, which are employed for high-voltage electricity distribution in urban areas. In presence of electrical current, those cables generate heat that has to be dissipated through the surrounding soil to keep the cable operating temperature at safety levels. The thermal behavior of buried cable is affected by the complex phenomenon of heat and moisture transfer in unsaturated soils. There is a vast literature on this subject and a good review can be found [1]. For a general discussion of the coupled problem of heat and mass transfer in porous medium reference is made to [2] or, most recently, [3].

All the works available in the literature dealing with

* Corresponding author

0017–9310/99/$ - see front matter
PII: S0017–9310(98)00322–6

transient heat and mass transfer in soil focus on a monotonic increase in the soil temperature due to the presence of a heated source. Representative examples are [4–6]. One recent exception is [7], where heat and mass transfer in the soil were modeled subject to a periodic heating.

The present paper presents for the first time an experimental investigation of the simultaneous heat and mass transfer in soils caused by a cyclic heat source. Computational results using the same methodology described in [7] are compared with the experiments, and general conclusions are offered.

2. Heat and mass transfer in soil

The equations that describe conservation of water (both liquid and vapor), and energy in moist soil are, respectively,

$$\partial\theta/\partial t = \nabla\cdot[D_{\theta w}\nabla\theta + D_{Tw}\nabla T - K_g\hat{k}] \quad (1)$$

and

$$C\partial T/\partial t = \nabla\cdot[\lambda^*\nabla T + \rho_l h_{lv} D_{\theta v}\nabla\theta] \quad (2)$$

where θ is the volumetric moisture content and T is temperature. Also, $\hat{k}$ is the unit vector in the gravity direction, ρ_l is the liquid density and h_{lv} is the latent heat of vaporization. The five phenomenological coefficients $D_{\theta w}$, D_{Tw}, K_g, C and λ^* depend on the moisture content and temperature, and reflect the major role played in heat and moisture transfer by three basic properties of the soil: suction potential, relative permeability and effective thermal conductivity. For each soil, the relationship between these basic properties with moisture content and temperature have to be determined experimentally. The coefficient $D_{\theta v}$ appearing in eqn (2) is related to the flux of vapor due to moisture content and together with the flux of liquid due to moisture content constitutes $D_{\theta w}$. Expressions for those coefficients are available in [7], and a detailed derivation of eqns (1) and (2) can be found in [1].

Equations (1) and (2) are highly nonlinear and strongly coupled to each other. They reflect that both heat and moisture migration are related to both temperature and water content gradients. The two most important phenomena for the situation under investigation here are the flux of vapor caused by heating (from higher to lower temperature regions) and the flux of liquid caused by moistening (from humid to dry regions). For underground power cables, a steady state situation is usually sought in which the flux of vapor away from the cable is counterbalanced by the flux of liquid towards the cable. Under extreme heating, a dryout region develops close to the cable. In turn, liquid continuity is interrupted precluding the return of moisture and causing what is called thermal instability of the surrounding soil.

As it will be seen later, eqns (1) and (2) together with their boundary conditions and the soil properties, can be used to successfully model the heat and mass transfer in soils.

3. Experimental setup

The experimental setup consisted of four parts: container, soil, heat source and instrumentation (including data acquisition).

3.1. Container

The container was a parallelepiped 1210 mm long, 865 mm wide and 639 mm high. Its top surface was opened to the ambient and the other five faces were made of asbestos. Those containers are commercially available and are commonly employed as domestic water reservoir. A plexiglass window, 0.5×0.2 m (length $\times$ high), was mounted in one of the lateral faces to allow a visual observation of the soil, indicating possible water vapor condensation.

An impermeable paint was used to cover the internal walls of the container precluding moisture transfer from the container to the surrounding air. To avoid a direct contact with the floor, a wooden frame separated the container from the ground, leaving a 15 mm layer of stagnant air. The top surface of the container was covered with a thin aluminum foil to reduce evaporation, and a 6 mm layer of the same soil used in the experiments was placed over the foil to minimize heat transfer. A 40 mm thick styrofoam layer was placed on the lateral sides of the container to reduce possible heat losses.

3.2. Artificial soil

The artificial soil employed here is a well-graded crushed granite stone, that is commonly used as a backfill material for underground cable installation. This backfill has 60% of its weight composed of gross grains having irregular shape of approximately 5 mm diameter and 40% composed of fine grains having 0.15 mm diameter. The material achieves its higher density of 2 g/cm^3 (porosity of 0.265) when compacted at 9% of moisture (in weight). All properties of this artificial soil are available in Oliveira [8], and some typical values are presented in Table 1. The apparent thermal conductivity, λ^*, shown in Table 1 was evaluated at 30% of saturation degree and 50°C, and the soil thermal diffusivity, α_d, is for 30% of saturation degree and 50°C.

3.3. Heat source

A copper tube having 25.4 mm external diameter and being 710 mm in length, with an electrical heater inserted in it, served as the heat source. The electrical heater is

Table 1
Typical properties of the artificial soil used in this work (from [8]) when compacted for porosity of 0.265

ρ_s (g/cm^3)	ρ_g (g/cm^3)	k_{sat} (m^2)	S_r	λ^* (W m^{-1} K^{-1})	α_d (m^2)
2.0	2.72	3.72×10^{-13}	0.04	1.6	8.42×10^{-7}

manufactured by Omega Inc., having 6.6 ± 0.127 mm internal diameter and being 711.2 mm$\pm1\%$ in length (heating zone of 597 mm). The thick wall of the copper tube together with a tight fit between the tube and the electrical heater assured both a uniform temperature and heat flux at the outer surface of the tube.

Figure 1 shows a schematic view of the heat source installed in the container, as well as a detailed view of the heat source. Figure 1b shows the two nylon-made supports that were used to attach the heat source to the container walls. The heat source laid horizontally along the container larger dimension.

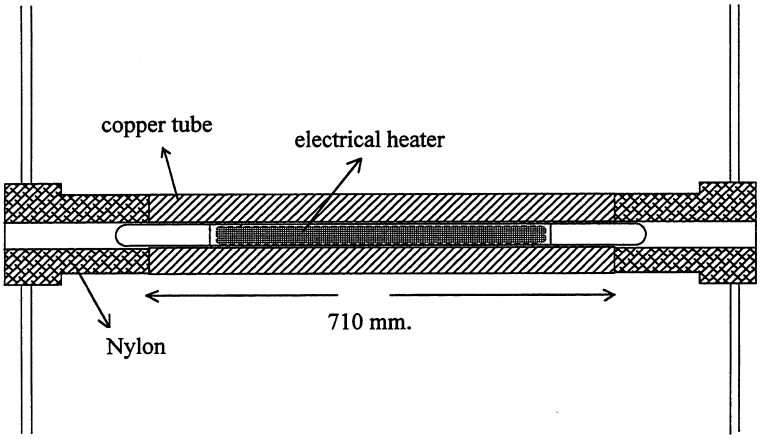

(a)

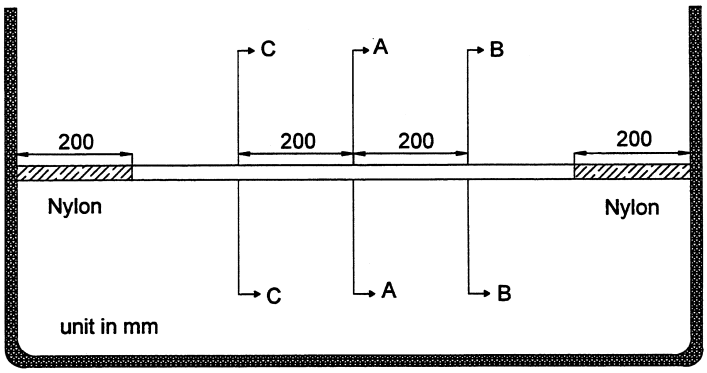

(b)

Fig. 1. Schematic view of the heat source installed in the container and detailed view of the heating cylinder.

3.4. Instrumentation

The quantities to be measured during an experimental run are temperature, soil moisture content and heat flux at the cylinder surface. All temperatures were measured using copper-constantan type T Omega thermocouples. Forty thermocouples were installed in three planes in the container (planes A, B and C indicated in Fig. 1); the thermocouple's number was limited by the number of channels available in the data acquisition system. For each plane the distances between the thermocouples were established using a logarithm scale, and their positions on plane A are shown in Fig. 2. The numbers in the figure correspond to the thermocouple distance to the center of the heated cylinder.

To measure the soil moisture content, use was made of tensiometers. These devices measure the soil suction potential and from that the moisture content was obtained. The tensiometer is constructed using a porous capsule connected to a pressure transducer. In the choice of the porous capsule there is a compromise between its time response and the suction pressure that it can measure. If the pores are very small the hydraulic resistance is large and the tensiometer response is slow. On the other hand, for large pores, a small suction pressure value can cause disruption of the hydraulic contact between the soil and the tensiometer affecting the capsule response. In the present case, use was made of a Soilmoisture capsule model 652×03-8143. It should be mentioned that the use of a pressure transducer instead of a U-type manometer avoids, for low moisture contents, an excess of liquid being transferred to the soil. That could result in a slow response of the device and an artificial soil moistening. A capacitive pressure transducer (Sensym model ST200), with a diaphragm and pressure range from -1 to 1 bar, was employed. Three tensiometers were located at places where drying and moistening were expected to occur at more intensity. Therefore, they were installed close to the heat source and at the bottom and lateral walls of the container. The number of tensiometers employed were much less than that of thermocouples due to possible disturbances in the soil because of their volume. While a thermocouple's junction was a sphere with less than 1.5 mm diameter, the tensiometer capsule has a cylinder-like shape having 6.35 mm diameter and 28.58 mm length. Distilled and deaerated water was employed in the tensiometer. Only one pressure transducer was employed and it was connected to the capsules through a system of hoses and valves.

Measurement of heat flux was directly made using heat flux sensors. A complete description of the heat flux sensors employed in the present work can be found in [9]. Basically, in those fluximeters the heat flux is measured along a tangential temperature gradient. The transducer is manufactured from copper and constantan in such a way that the heat flow is deviated establishing a temperature gradient perpendicular to the transducer surface. Five transducers were used for monitoring the

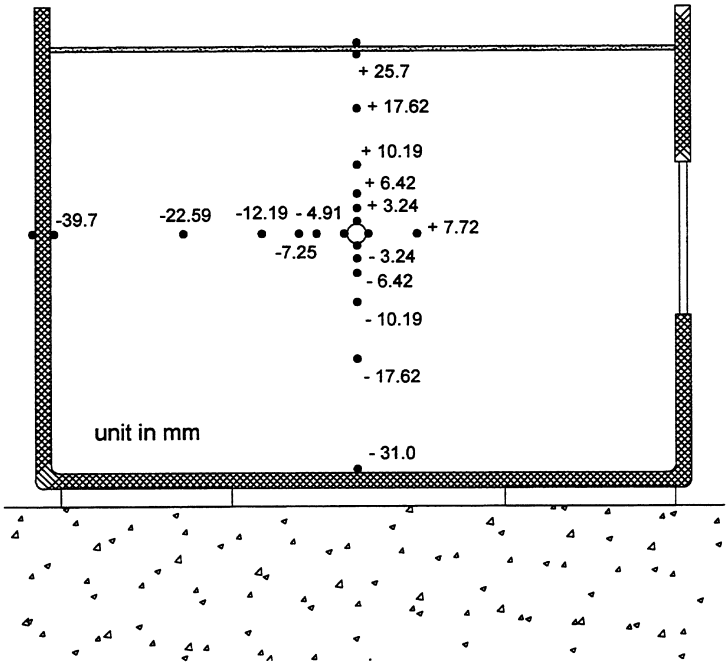

Fig. 2. Thermocouples location on plane A according to Fig. 1.

heat flux from the heated cylinder. Four of them were installed at the same vertical plane (20 mm to the right of plane A in Fig. 1), equally distributed along the circumference of the heated cylinder. The fifth transducer was placed close to the nylon support to check for the non-uniformity of the heat flux along the cylinder axis. The fluximeters were specially manufactured for the present experiment. An important feature of them was their curvature that coincided with that of the cylinder, assuring a perfect contact between the surfaces. Details related to calibration of all the instrumentation used in the experiment can be found in [10].

A data acquisition/control Hewlett–Packard system was employed to monitor the signals from the 40 thermocouples, five fluximeters and one pressure transducer. The system was operated via a microcomputer that stored and processed the data.

To monitor and control the power dissipated by the heat source a dc power supply and a digital multimeter were employed, both connected in series with the electrical heater.

4. Experimental preparation and procedure

In preparing the experiments, particular attention was devoted to assure a uniform compactation of the soil in the container. To that extent the container was carefully leveled and metallic tapes with a millimeter scale on them were placed at each one of the container's corners. Because the container walls were not flat for structural reasons, water was poured in it and a curve of volume vs the height measured by the matallic scales was obtained. This curve was used in compacting the soil in the container.

Before the soil was placed inside the container, 30 kg of dry soil was mixed with 1.3 kg of water. After the soil was compacted to a porosity of 0.27, this amount of water resulted in a soil saturation degree (volume of water divided by volume of pores) of 30%. In the sequence, the material was well mixed and 20 kg of it was then separated and placed in the container for compactation. The four metallic tapes assured that the level of soil within the container was kept uniform during the compactation of each layer. At the end of the process, when the container was filled with the artificial soil, the overall density achieved was 1956.5 kg/m^3, which corresponded to a porosity of 0.27, as desired.

The installation of the heated cylinder, thermocouples, heat flux sensors, and tensiometer capsules, were all made as the container was being filled. All thermocouples were laid in the plans parallel to the cylinder axis to minimize fin effects. The thermocouples used to read the temperatures of the heated cylinder were attached to the cylinder surface and their junctions were placed with thermal paste in small holes 1.5 mm diameter.

One of the tensiometers was installed in plane A (Fig. 1) touching the surface of the heated cylinder; the other two were located on plane A close to the bottom of the container and on the cylinder horizontal plane close to the plexiglass window.

5. Experimental results and discussion

Before the heat source was activated for the first time, the tensiometers indicated 0.425 bar of suction pressure, which corresponds to a soil saturation degree of 30%. This value is in agreement with the amount of water mixed with the soil during the preparation of the experiment. For this soil, a saturation degree of 30% corresponds to a funicular state; that is, a situation where liquid continuity prevails. The critical moisture content of the present soil is 4%, and below this value the liquid within the pores is immobile (pendular state) precluding the occurrence of a liquid flux due to capillary. The chosen value of 30% of saturation degree is in between a condition of dry and humid soil and was expected to yield an interesting behavior of the moisture migration in the vicinity of the heated cylinder.

Another aspect observed before the cylinder was heated was the instantaneous response of the soil temperature to small variations of the surrounding air temperature. That is true for all thermocouples, regardless of their location. The important conclusion that can be drawn from this observation is that, truly speaking, the soil cannot represent an infinite medium regarding the transient heat transfer from the cylinder, as would be desired. Even for short times after the heat source is activated, the boundaries of the container affected the soil temperature. This is not a dominant effect since the temperature of the heating cylinder reached values considerably higher than both the soil initial temperature and the ambient air temperature. However, in calculating the soil temperature using the numerical model, the actual time-dependent temperatures of the container boundaries have to be employed; further comments on that will be made when considering the numerical model.

The experimental results to be explored are divided in two categories: constant and periodic heat flux. For constant heat flux four situations were investigated: 8, 17, 42 and 80 W m^{-1}; for periodic heat flux, the power dissipated was kept equal to 42 W m^{-1}, and cycles of 6 and 12 h were explored.

5.1. Constant heat flux

Results for heat flux constant and equal to 17, 42 and 80 W m^{-1} are presented in Figs 3–5 for the vertical thermocouples located on plane A of Fig. 1. In those figures, each curve corresponds to the time variation of the temperature for a given thermocouple. In addition to

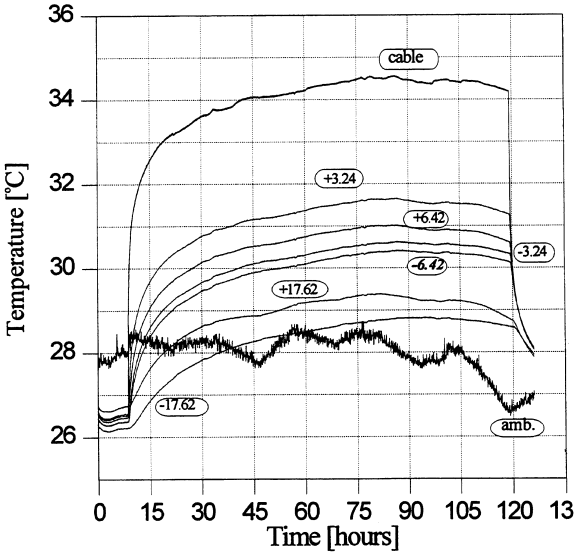

Fig. 3. Variation with time of the soil temperature at different vertical locations for 17 W m^{-1}; plane A in Fig. 1.

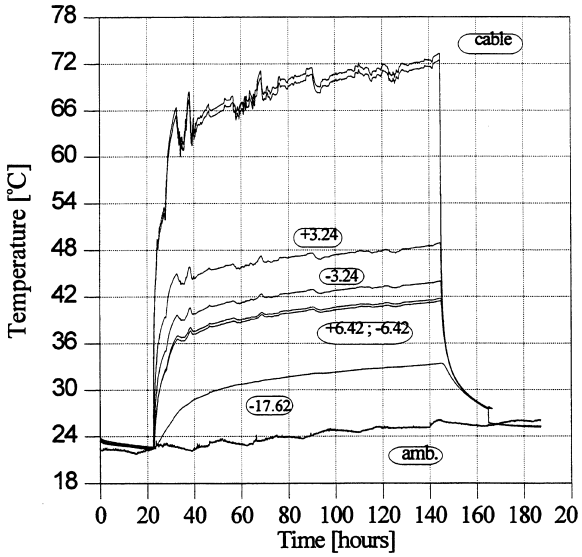

Fig. 5. Variation with time of the soil temperature at different vertical locations for 80 W m^{-1}; plane A in Fig. 1.

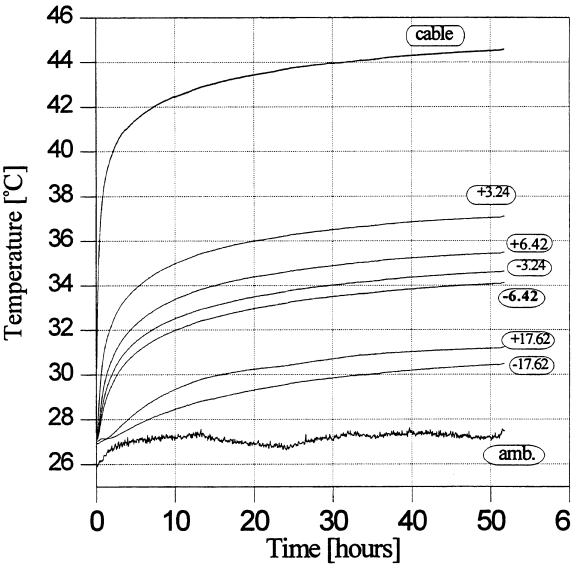

Fig. 4. Variation with time of the soil temperature at different vertical locations for 42 W m^{-1}; plane A in fig. 1.

the temperature at the cylinder surface, and the ambient temperature, results for six other locations are presented. The exact location associated to each thermocouple installed in the soil is shown by the number close to the curve; a positive number indicates a location above the cylinder whereas a negative number is for locations below the cylinder. Thermocouple + 17.62 in Fig. 5 is not shown because its wire was broken during the compactation of the soil.

The first thing to be observed in Figs 3–5 is that once the heat source is activated, all thermocouples in the soil feel the heating effect. After an initial period of heating, there is a tendency for thermal stabilization in which the temperature of all thermocouples does not vary with time; at this period the soil temperature is only affected by variations of the ambient temperature. The closer to the cylinder is the soil, the higher is its temperature, as expected. However, contrary to the one dimensional pattern that would be expected (temperature function of the radial distance only), the thermocouples located above the heated source indicated temperatures higher than those below the source. It was observed that for the same location, the difference between the temperature above and below the cylinder on a vertical plane increased as the heat flux increased. For location 3.24 cm on plane A, for example, the differences of 8, 17, 42 and 80 W m^{-1} were, respectively, 0.54, 1.1, 2.5 and 4.9°C. It is believed that those differences are due to a nonuniform heat flux on the cylinder related to the soil compactation adjacent to its surface, as will be explored later.

For the heat flux of 80 W m^{-1}, ripples are observed on the response of the thermocouples close to the heated cylinder due to instabilities of the power supply. At the cable surface the ripples have amplitude as high as 1.5°C. Due to limitations of the power supply used for the lower heat fluxes, for the higher heat flux another less stable power supply (Tectral model 50-05) was employed.

As indicated in Fig. 3 for time equal to 120 h, and Fig. 5 for 145 h, the heat source was eventually deactivated and all temperatures started to drop. Again, the soil response to this change in the boundary condition was

very fast. This deactivation prevented the effect of the boundaries of the container to affect the soil temperature and moisture content close to the cylinder, and allowed an investigation of how the soil responded to an abrupt discontinuity on the power supply.

Figures 6–8 present for 17, 42 and 80 W m^{-1}, respectively, the temperature variation as a function of the horizontal radial distance, for the thermocouples on plane A of Fig. 1. The number close to each curve indicates the time at which the measurements were taken. As mentioned before, the origin is located at the axis of the heated cylinder. The positive values of the radial distances indicated in those figures correspond to one side of the cylinder and the negative value to the other side. The thermocouples on the left most side of Figs 6–8 indicate the soil temperature at the container wall. Interruption of the experimental runs after certain time always occurred due to interferences of the container boundaries on the transient process occurring in the soil, as seen from the figures.

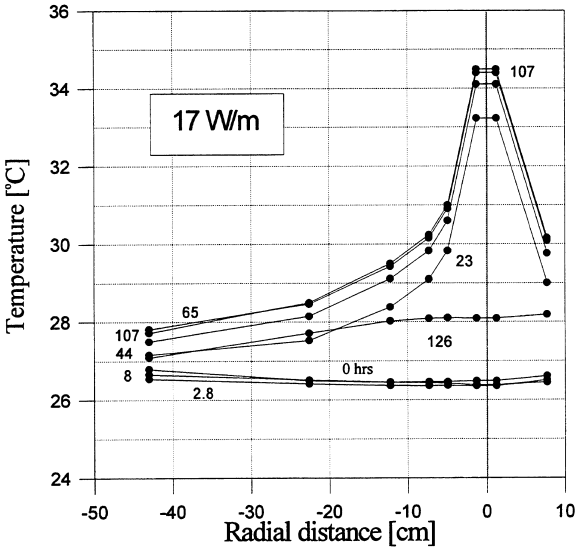

Fig. 6. Temperature variation as a function of the radial distance for 17 W m^{-1}; plane A in Fig. 1.

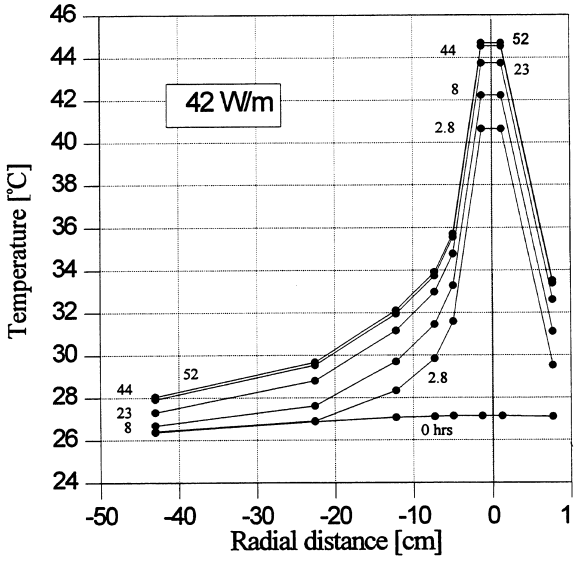

Fig. 7. Temperature variation as a function of the radial distance for 42 W m^{-1}; plane A in Fig. 1.

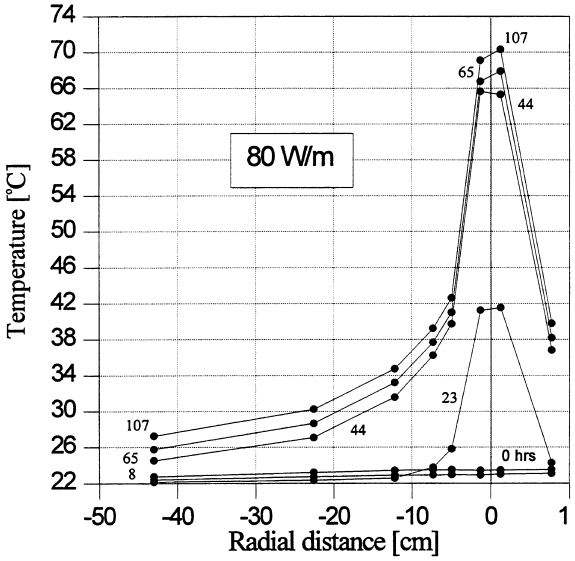

Fig. 8. Temperature variation as a function of the radial distance for 80 W m^{-1}; plane A in Fig. 1.

The thermocouples located on planes B and C shown in Fig 1 indicated temperatures slightly lower than those of plane A. The difference between plane A and plane B and C increased as the heat flux increased but never reached more than 1.5°C. Those differences are due to tridimensional effects of the container geometry.

5.2. Periodic heat flux

Results for the periodic heat flux will now be explored. As explained before, the heat flux was kept equal to 42 W m^{-1} and cycles of 6 and 12 h will be presented. Figure 9 corresponds to a cycle in which the source remained activated during 6 h and deactivated for the next 6 h; after that the cycle was repeated. Figure 10 corresponds to cycles of 12 h. Both figures show the thermocouples located on plan A of Fig. 1, aligned along a vertical line perpendicular to the cylinder axis and passing through its center.

From the figures it is seen that during both the heating and non heating periods, the soil responds rapidly to the

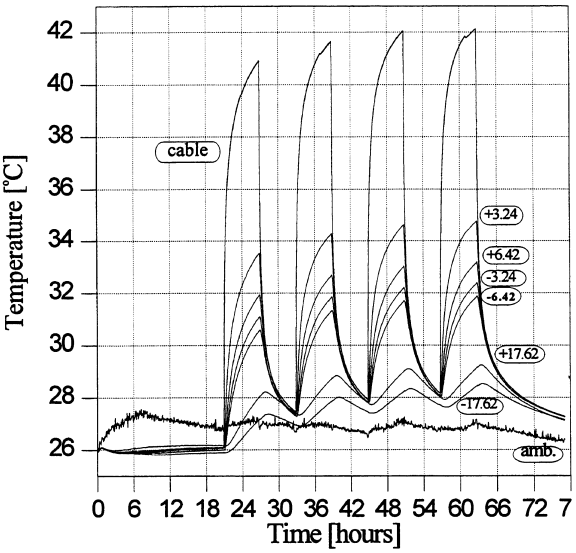

Fig. 9. Variation with time of the soil temperature at different vertical locations on plane A of Fig. 1; heat flux of 42 W m^{-1} in periodic cycles of 6 h.

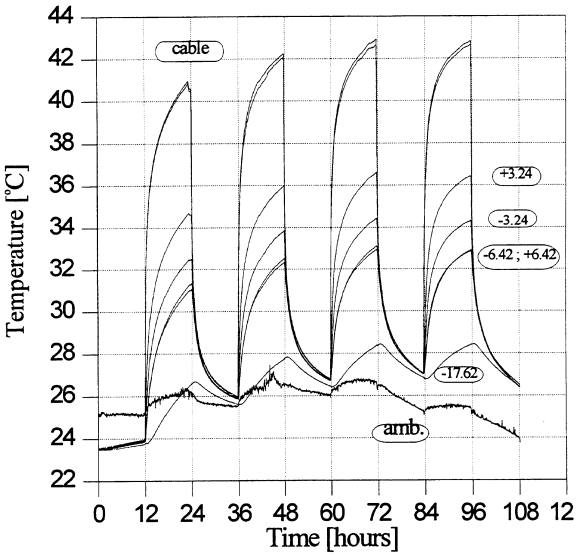

Fig. 10. Variation with time of the soil temperature at different vertical locations on plane A of Fig. 1; heat flux of 42 W m^{-1} in periodic cycles of 12 h.

power variation. This is particularly true for the thermocouples near the cylinder. As the distance from the cylinder increases, a time lag is observed. For the thermocouple located at ± 17.62 cm from the cylinder, there is a delay of about 1 h before the temperature starts to decrease, once the source is deactivated.

Another aspect to be observed from Figs 9 and 10 is that the temperature response for both figures presents a very similar pattern. For both heating periods, the periodic regime is established after three cycles and the cable temperatures obtained in both cases are very close, that is, 42 and 43°C for the 6 and 12 h cycle, respectively. It should be mentioned that, despite the different heating cycle, the good agreement observed between Figs 9 and 10 can be used to assess the experiment reliability. This is so because the results of Fig. 10 were obtained after the whole setup was disassembled and the experimental procedure and preparation was repeated, including the soil compaction and positioning of the instrumentation.

Also observed from Figs 9 and 10 is the difference between the soil temperature above and below the cylinder at the same radial distance. As mentioned before, this small but noticeable effect is believed to be caused by a nonuniform heat flux boundary condition, as will be explored in the next paragraph.

5.3. Heat flux sensors

In general the results obtained from the heat flux sensor corroborated those monitored by the power supply and the digital multimeter. For a heating power of 42 and 80 W m^{-1}, the average value of the three fluximeters located on the top and on the sides of the cylinder surface registered 41 and 84 W m^{-1}, respectively. However, the fluximeter located on the bottom of the heated cylinder indicated values considerably lower than the other three: 20 and 50 W m^{-1} for the power supply of 42 and 80 W m^{-1}, respectively. Several attempts were made to rationalize this discrepancy. One possible explanation is that during the compactation of the soil, a thin air layer always remained beneath the cylinder because of the difficulty in accessing this region. Calculations indicated that for a 0.5 mm air layer between the cylinder and the adjacent soil, the local heat flux on the bottom surface is reduced by 50% compared to the heat flux on the top surface. Because of the high thermal conductivity of the copper, nonuniformities of the surface were not detected by the thermocouples. It is possible that this nonuniformity on the heat flux could have had some effect on the temperature field in the soil surrounding the cylinder. In this regard, the temperature difference observed between points above and below the cylinder, but at the same radial location it is believed to be caused by the nonuniform heating.

The heat flux sensor placed close to the nylon support (see Fig. 1) indicated a heat flux value 9% lower than the ones located at the central part of the container. Again, this is an indication of some tridimensional effects.

5.4. Moisture content

Measurements of the moisture content for a heat flux of 42 W m^{-1} indicated that close to the cylinder surface

the saturation degree was 23%. Close to the container wall the saturation degree remained around 30%. The measurement of the moisture content using the tensiometers were troublesome and the quality of the data was not good. Even using a pressure transducer instead of a U-type manometer, and a capsule with low hydraulic resistance, the response was too slow and 5 h were required to obtain a suction pressure of 0.4 bar. This is a short time when compared to the 24 h required if a U-type manometer was employed, but still is a long time for the type of situation investigated here. Furthermore, because of the relative large size of the pores in the capsule (needed to yield a low hydraulic resistance), very often air bubbles appeared in the hose that connected the capsule to the pressure transducer, indicating that the continuity of the liquid phase had been disrupted. For instance, the 23% of saturation degree observed near the heated cylinder for a heat flux of 42 W m^{-1} corresponded to a suction pressure of 0.65 bar, and at this pressure level air bubbles started to appear. All that precluded measurement of moisture contents for the heat flux of 80 W m^{-1}.

5.5. Dimensionless temperature

To place the results for the temperature at the cylinder surface under perspective, data for all heat fluxes were combined in Fig. 11. In preparing the figure, both temperature and time were made dimensionless using the following quantities,

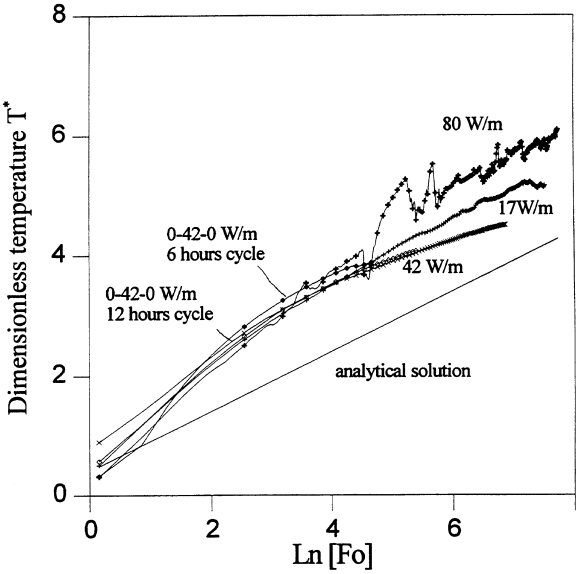

Fig. 11. Variation of the dimensionless temperature at the cylinder surface with the dimensionless time for different heat fluxes.

$$T^* = 2\pi\lambda^*(T - T_i)/q', Fo = \alpha_d t/r_c^2 \quad (3)$$

where λ^* is the soil apparent thermal conductivity at 50°C and saturation degree of 30% ($=1.69$ W m^{-1} K^{-1}), T_i is the initial temperature of the soil before the heat source is activated, q' is the heat flux per unit length, α_d is the soil thermal diffusivity at 50°C and saturation degree of 30% ($=8.42\times10^{-7}$ m^2 s^{-1}) and r_c is the cylinder radius.

Results for both the constant and periodic heat fluxes are plotted in Fig. 11. For the periodic heat fluxes, only the heating period is indicated. Also shown in the figure is the analytical one-dimensional solution for the conduction equation with constant properties.

The first thing to be noted in Fig. 11 is that all experimental results seem to correlate for ln(*Fo*) less than 5, which for the present situation corresponds to less than 8 h. After this time the curves start to deviate one from the other. The role played by moisture migration can be seen by comparing the one-dimensional analytical solution with the experimental results. As seen from the figure, all experimental results lie above the analytical solution, indicating that, because of the heating, the soil thermal conductivity near the cylinder decreases, resulting in a higher temperature of the cylinder surface. Also noted is that at earlier times the derivatives of the temperatures for the experimental results tend to increase as time progresses, and later start to either decrease or remain constant. One possible explanation for this behavior is that after the heat source is activated, the heating of the soil causes a moisture migration away from the cylinder decreasing the soil thermal conductivity. Once the moisture migration is stopped, because the vapor flux aligned with the heat flux is counterbalanced by the liquid flux on the opposite direction due to capillarity, the thermal conductivity becomes constant. The decrease in the derivative of the temperature 42 W m^{-1} is somehow unexpected, particularly because the curve associated with this heat flux lies below the heat flux of 17 and 80 W m^{-1}; no explanation for this was found.

The cylinder dimensionless temperatures for cycles of both 6 and 12 h are plotted in Fig. 12. It is seen from the figure that, despite some deviations before the heat source be both activated and deactivated, both curves are very similar. The temperature at the cylinder presents the same behavior with time regardless the duration of the heating cycle.

6. Comparison between experiment and computation

The heat and mass transfer in soils can be described by eqns (1) and (2), as discussed before. For the present situation those equations were solved using a finite volume methodology according to [11–12]. The container was divided into small nonoverlapping control volumes, and the eqns were integrated over each one of the control

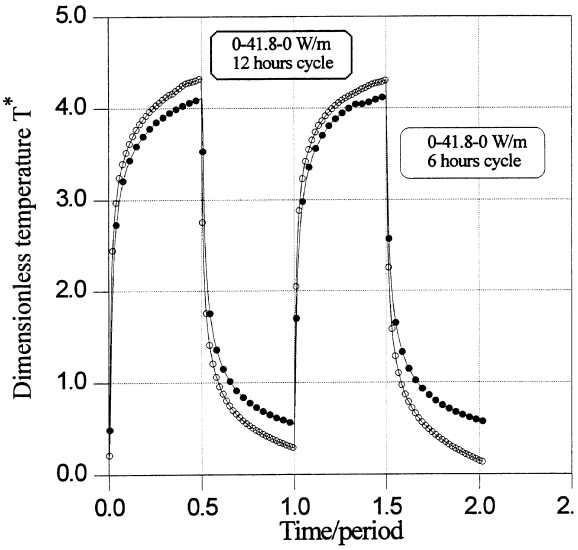

Fig. 12. Cylinder dimensionless temperature for both 6 and 12 h of heating cycle.

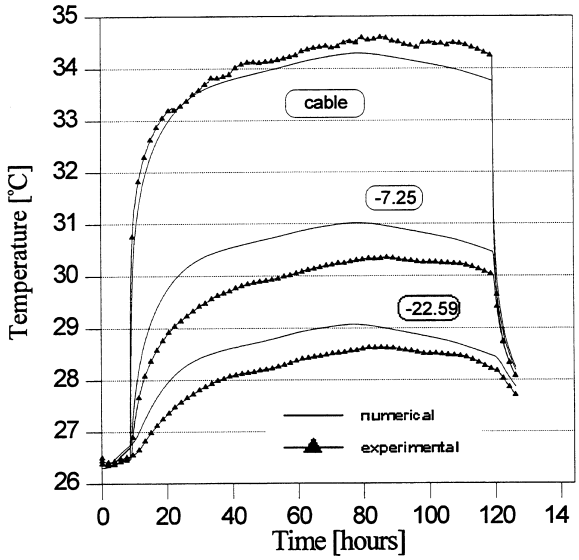

Fig. 13. Comparisons between numerical and experimental results for the temperature at different horizontal locations on plane A of Fig. 1; heat flux of 17 W m^{-1}.

volumes. Cartesian coordinates were employed as recommended by [7]. The effect of this simplification was tested comparing the results obtained using the present approach with the analytical solution of the one-dimensional conduction equation for constant properties. Only the isotherms very close to the cable were distorted by the use of cartesian mesh and the maximum deviation observed in the cable temperature was 0.2°C.

For the boundary conditions, the actual time-dependent temperatures at the container's boundaries were prescribed and all surfaces were assumed to be impermeable. Symmetry was adopted and then only half of the domain was considered. The computational domain was discretized using 24 control volumes along the horizontal direction and 38 on the vertical direction. The mesh was refined closer to the heated cylinder to capture the higher gradients therein. A fully implicit scheme was employed for the time discretization. Because of the large computer time required to solve eqns (1) and (2) due to the strong dependence of the soil properties with moisture content and temperature, the computational mesh represented a compromise between numerical accuracy and computer time. A detailed description of the numerical solution of eqns (1) and (2) is beyond the scope of the present work and for more information on that, reference is made to [7] and [10].

6.1. Constant heat flux

Results for the evolution with time of both temperature and moisture content are presented in Figs 13 and 14, respectively, for a heat flux of 17 W m^{-1}. For the moisture content, only the numerical results are shown because of

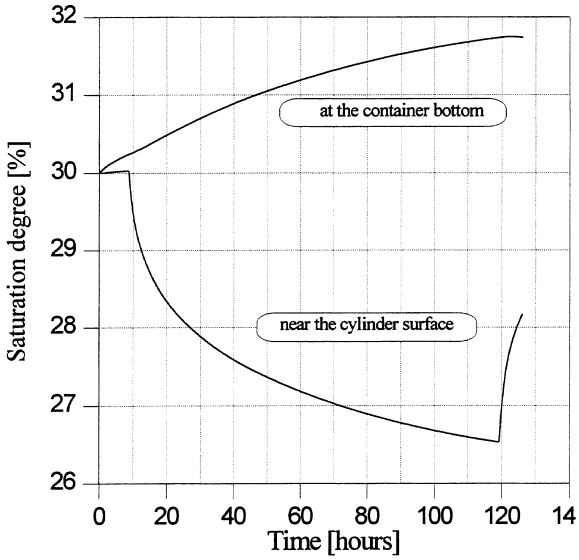

Fig. 14. Variation with time of soil saturation degree close to the cylinder and at the bottom of the container for a heat flux of 17 W m^{-1}.

the already mentioned difficulty in obtaining reliable data with the tensiometer. Despite the deviations between experiment and computation as observed in Fig. 13, a good agreement prevailed. An interesting result observed from Fig. 14 is the great capacity of this type of soil in sucking water from the medium; as shown in the figure, for time equal to 120 h, as soon as the heat source is

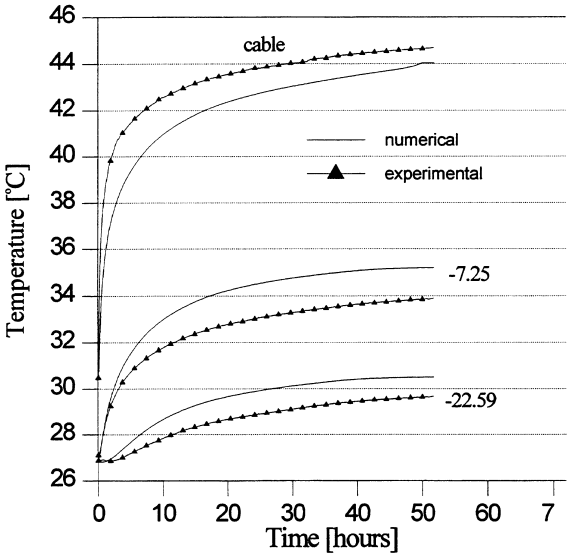

Fig. 15. Comparison between numerical and experimental results for the temperature at different horizontal locations on plane A of Fig. 1; heat flux of 42 W m^{-1}.

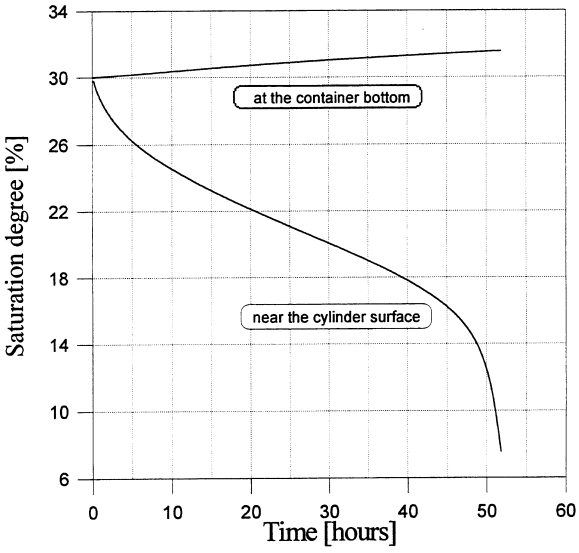

Fig. 16. Variation with time of soil saturation degree close to the cylinder and at the bottom of the container for a heat flux of 42 W m^{-1}.

deactivated and the temperature gradient is stopped, the soil near the cylinder sucks water back increasing its saturation degree. The computations also revealed an existing asymmetry of the moisture field along the vertical (this effect is not visible from Fig. 14). Because of the gravity, moisture at the lower part of the container was always higher than at the upper part.

Results for temperature and moisture content corresponding to a heat flux of 42 W m^{-1} are presented in Figs 15 and 16, respectively. Again, the numerical solution was able to predict the variation of temperature with time with a reasonable to good accuracy. The moisture content close to the cylinder for this level of heat flux was much lower than the one observed before for 17 W m^{-1}; as seen from Fig. 16, a very low moisture degree was found to exist near the heated cylinder, reaching values as low as 8%. Results for a heat flux of 80 W m^{-1} (not shown here) indicated that for such a flux the moisture content at the cylinder goes to zero drying the soil completely. However, the drying region is restricted to a very close region near the cylinder and 4 cm away from it the saturation degree is already 22%. This reflects the great capacity of such a well-graded soil in retaining the moisture even in presence of a strong temperature gradient. That is a behavior completely different from what is observed in uniform graded sand, for instance, that tend to dry under little thermal stress, as seen in [13].

6.2. Periodic heat flux

Attention is now turned to the periodic heat flux and to this extent Figs 17 and 18 were prepared. Figure 17

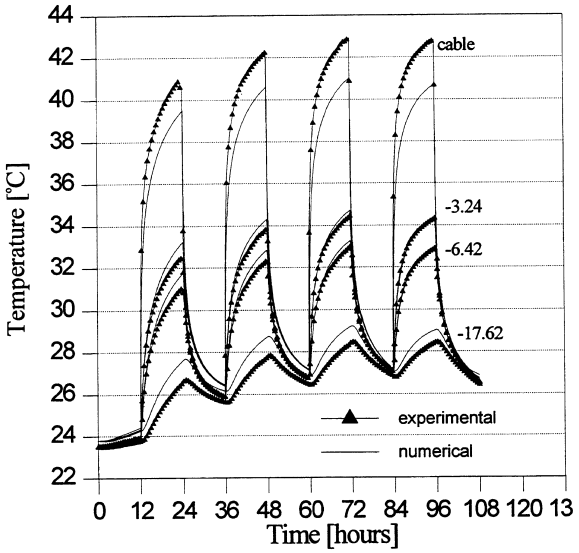

Fig. 17. Comparison between numerical and experimental results for the temperature at different vertical locations on plane A of Fig. 1; heat flux of 42 W m^{-1} in periodic cycles of 12 h.

shows the comparison between experiment and computation for a heat flux of 42 W m^{-1} with 12 h of heating cycle. In general, a good agreement is observed between the model and the data with larger deviations for the cylinder temperature. The results for the soil saturation degree as observed in Fig. 18, indicates that the moisture content near the cylinder follows the same periodic pattern observed for the temperature and imposed by the

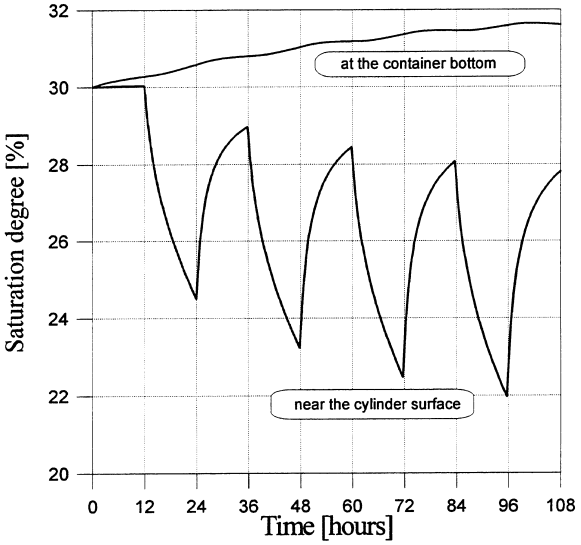

Fig. 18. Variation with time of soil saturation degree close to the cylinder for a heat flux of 42 W m^{-1} in periodic cycles of 12 h.

heat flux. When the heat flux is activated, moisture is pushed away from the cylinder due to vapor flux; when the source is deactivated and the vapor flux is stopped, capillary sucks liquid back to the cylinder.

For all cases investigated, the measured temperature at the heated cylinder is consistently higher than the predicted one while everywhere else the predicted temperature is higher than the experimental results. The explanation for that should be related to the strong dependence of the soil thermal conductivity with the moisture content and the difficulty in predicting this dependence. When the soil thermal conductivity is artificially altered (increased close to the cylinder and decreased away from it) the deviations between experiments and computations both at the heated cylinder and away from it can be reduced and the aforementioned tendency can be changed.

7. Final remarks

Both the experimental and the numerical results have shown that for the type of soil explored in the present work and the range of parameters investigated, the role played by the moisture field is in affecting the thermal conductivity of the soil rather than in transferring energy due to water migration. Little difference was observed in the numerical model when only the conduction equation was solved (results not shown here). For those simulations the only care that had to be taken was to use a thermal conductivity of 1.47 W m^{-1} K, which is a value smaller than that corresponding to the initial saturation degree of the soil, that is, 1.69 $W.^{-1}$ K. Those findings are in agreement with previous works where it was observed that the conduction equation with moist-dependent thermal conductivity is adequate to determine the temperature distribution [5]. Except for situations where a large drying region occurs near the heated cylinder [7], there is no need to solve both the energy and moisture equation coupled.

References

[1] J.A.G. Hartley, Coupled heat and moisture transfer in soils: a review, in: A.S. Mujumdar (Ed.), Advances in Drying, Hemisphere Publishing Co., New York, 1987, pp. 199–248.
[2] S. Whitaker, Simultaneous heat, mass and momentum transfer in porous media. A theory of drying, in: J.P. Harnett, T.F. Irvine Jr., (Eds), Advances in Heat Transfer vol. 13, 1977, pp. 119–200.
[3] Bories, S.A., Fundamentals of drying of capillary-porous bodies, in: Convective Heat and Mass Transfer in Porous Media, Kluwer Academic Publishers, The Netherlands, 1991, pp. 391–434.
[4] J.Y. Baladi, D.L. Ayers, R.J. Schoenhals, Transient heat and mass transfer in soils, International Journal of Heat and Mass Transfer 24 (1981) 449–458.
[5] J.A.G. Hartley, W.Z. Black. Transient simultaneous heat and moisture transfer in moist unsaturated soils. ASME Journal of Heat Transfer 103 (1981) 376–382.
[6] J. Ewen, Thermal instability in gently heated unsaturated sand. International Journal of Heat and Mass Transfer 31 (1988) 1701–1710.
[7] D.S. Freitas, A.T. Prata, A.J. Lima. Thermal performance of underground power cables with constant and cyclic currents in presence of moisture migration in the surrounding soil, IEEE Transactions of Power Delivery 11 (1996) 1159–1170.
[8] A.A.M. Oliveira Jr., Characterization of the thermo-hydraulic properties of artificial materials for buried power cables (in Portuguese), M.Sc. Thesis, Federal University of Santa Catarina, Brazil, 1993.
[9] S. Güths, Anemomètre à effet peltier et fluxmètre thermique: conception et réalisation. Application a l'étude de la convection naturelle, Dr Thesis, Université D'Artois Pôle Béthune, France, 1994.
[10] R.E.S. Moya, Experimental analysis in unsteady periodic regime of heat and moisture transfer around a buried power cable (in Portuguese), Dr Eng. Thesis, Federal University of Santa Catarina, Brazil, 1996.
[11] S.V. Patankar, Numerical Heat Transfer and Fluid Flow, Hemisphere Publishing Co., New York, 1980.
[12] J.H. Ferziger, M. Peric. Computational Methods for Fluid Dynamics, Springer-Verlag, Berlin, 1996.
[13] J. Ewen, Susceptibility to drying of unsaturated soil near warm impermeable surface, International Journal of Heat and Mass Transfer 33 (1990) 359–366.